

Peak Separation by Derivative Spectroscopy Applied to FTIR Analysis of Hydrolized Silica

Bernardo J. G. de Aragão*^a and Younes Messadeg^b

^a Fundação CPqD, Rod. SP 340 Campinas-Mogi Mirim, km 118, 13086-902 Campinas-SP, Brazil

^b Instituto de Química, Universidade Estadual Paulista, R. Francisco Degni s/n, 14800-900 Araraquara-SP, Brazil

Supplement 1: Analysis of Spectrum 1 (Unaged fiber)

Shoulder and detection limit maps

From the data of Table 2 and Table 4 of the original paper follows the calculation of the values of R, φ and δ , which are given in Table S1.

Table S1. Values of R, φ and δ

Overlapping peaks/ (cm ⁻¹)	δ	R	φ
3635.46/3475.96 ^a	1.89	0.87	1.7
3475.96/3284.95 ^{a,b}	1.75	0.61	1.0
3284.95/3122.90 ^{a,b}	2.18	0.25	1.6
3675.50/3612.15 ^b	1.18	0.53	1.2
3612.15/3475.96 ^b	1.81	0.79	1.7

^a Valid for Model I and ^bValid for modified Model I.

Figure S1 shows the shoulder limit map for the field aged fibers. The Model I is analyzed from (a) to (c). The 3635.46/3475.96 cm⁻¹ overlapping peaks (a) are just over the shoulder limit (the limiting line for $\varphi = 1.7$ lies between $\varphi = 1.6$ and $\varphi = 1.8$), which means that they can still be visually distinguished. All other pairs of overlapping peaks ((b) and (c)) cannot do so, since they are under the shoulder limit. This is confirmed by Figure 4 of the paper.

Using the modified Model I, the peak at 3635.46 cm⁻¹ is substituted by two peaks at 3675.50 and 3612.15 cm⁻¹ which are not visually resolved (Figure S1 (d) and (e)). It is interesting to note that the 3612.15/3475.96 cm⁻¹ overlapping peaks are beyond the detection limit but do not show up in the second derivative. The reason is that the 3612.15 cm⁻¹ peak cannot be detected separately from the 3675.50 cm⁻¹ peak, as shown in Figure S2.

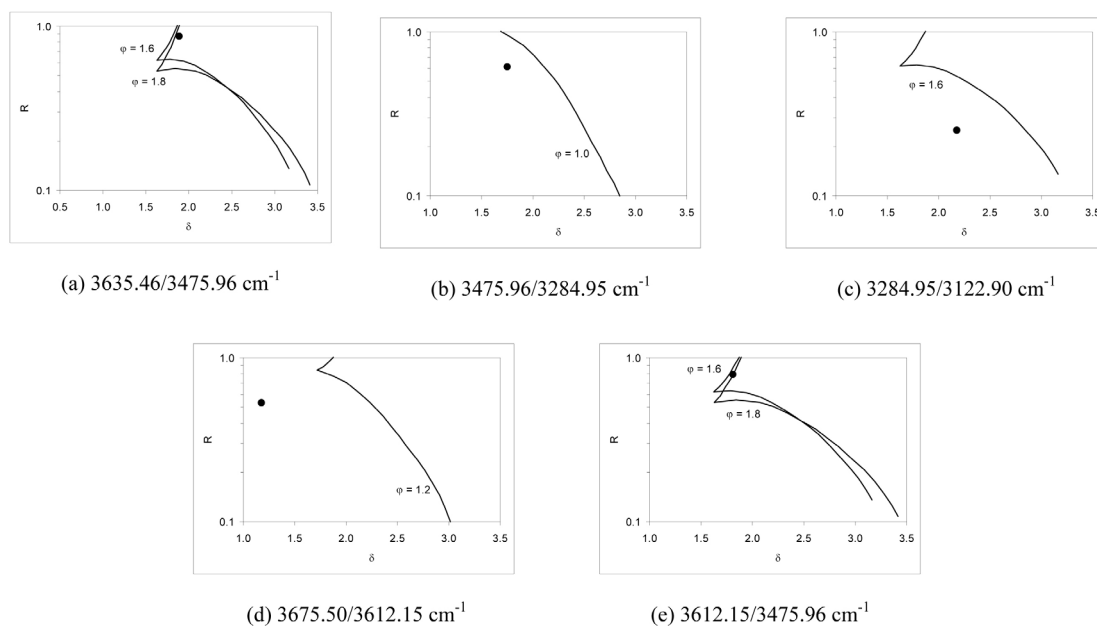


Figure S1. Shoulder limit.

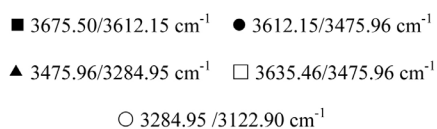
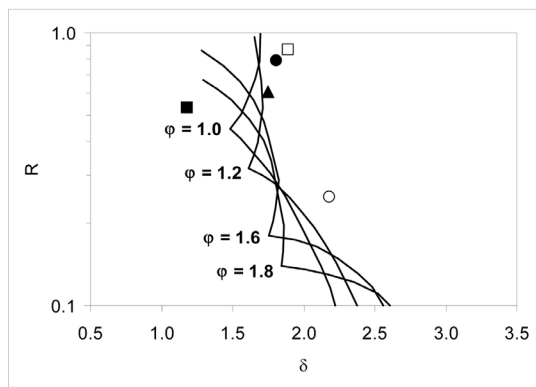


Figure S2. Detection limit.

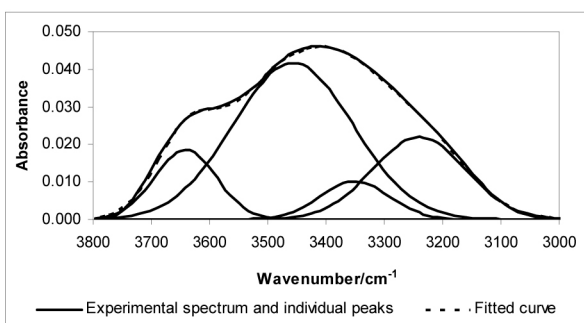
Supplement II: Analysis of Spectrum 2 (Field aged fiber)

Curve fitting according to Model I to IV

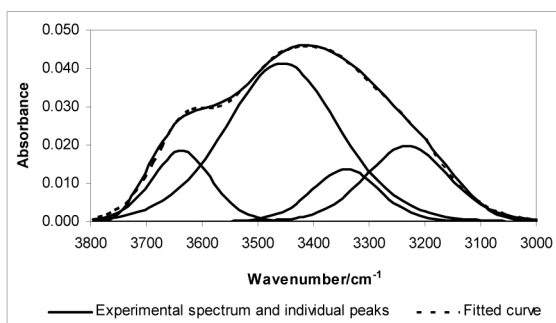
From Model I to Model III, differences were observed mainly in peak height at 3340 and at 3200 cm^{-1} . Model IV yielded the worst fit (Figure S3). The numerical results are given in Table S2.

Shoulder and detection limit maps

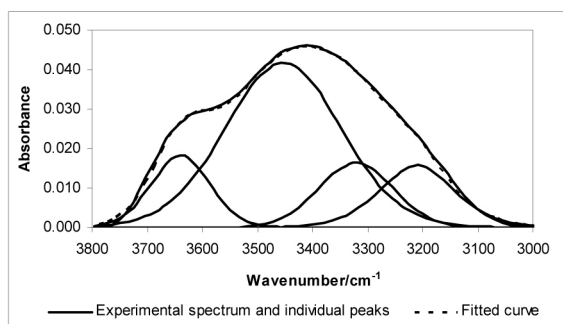
From the data of Table S2 and Table 7 of the original paper follows the calculation of the values of R , ϕ and δ , which are given in Table S3.



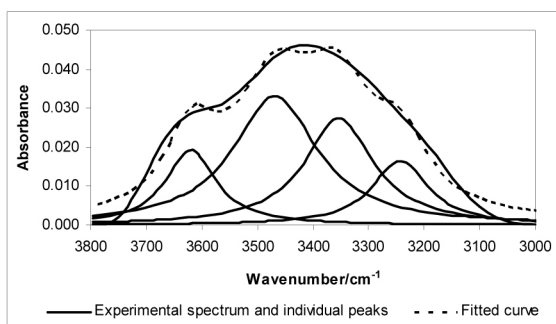
(a) Model I



(b) Model II



(c) Model III



(d) Model IV

Figure S3. Curve fitting results.

Table S2. Numerical results of curve fitting

Initial guess for peak maximum	Parameter	Model I	Model II	Model III	Model IV
3640 cm ⁻¹	v ₀ (cm ⁻¹)	3641.28	3637.10	3639.35	3619.23
	A	0.0186	0.0185	0.0182	0.0193
	s (cm ⁻¹)	75.25	101.06	90.00	55.09
	s' (cm ⁻¹)	-	-	132.53	-
3450 cm ⁻¹	v ₀ (cm ⁻¹)	3456.64	3455.89	3453.11	3468.41
	A	0.0416	0.0414	0.0417	0.0330
	s (cm ⁻¹)	145.52	193.93	173.21	92.07
	s' (cm ⁻¹)	-	-	274.09	-
3340 cm ⁻¹	v ₀ (cm ⁻¹)	3350.13	3341.63	3320.92	3353.53
	A	0.0102	0.0138	0.0164	0.0275
	s (cm ⁻¹)	83.64	114.48	100.00	75.06
	s' (cm ⁻¹)	-	-	349.82	-
3200 cm ⁻¹	v ₀ (cm ⁻¹)	3240.04	3231.77	3210.50	3242.51
	A	0.0220	0.0198	0.0158	0.0164
	s (cm ⁻¹)	113.05	142.92	141.42	61.81
	s' (cm ⁻¹)	-	-	117.38	-

^aUnit (cm⁻¹), v₀ - peak maximum, s - peak width and s' - the bandwidth term of the Lorentzian part, except A. A - peak height.

Table S3. Values of R, φ and δ

Overlapping peaks (cm ⁻¹)	δ	R	φ
3641.28/3457.25 ^a	2.24	0.45	1.9
3680.53/3622.16 ^b	1.17	0.42	1.4
3622.13/3457.25 ^b	2.09	0.42	1.9
3457.25/3319.49 ^{ab}	1.42	0.53	1.3
3319.49/3204.75 ^{ab}	1.41	0.70	1.1

^a valid for Model I, ^b valid for modified Model I.

Figure IV shows the shoulder limit map for the field aged fibers. The Model I is analyzed from (a) to (c). The 3641.28/3457.25 cm⁻¹ overlapping peaks (A) are under but close to the shoulder limit (the limiting line for φ = 1.9 lies between φ = 1.8 and φ = 2.0), which means that they are close to the limit of visual distinction. All other pairs of overlapping peaks ((b) and (c)) cannot be visually distinguished, since they are under the shoulder limit. This is confirmed by Figure 7 of the paper. The overlapping

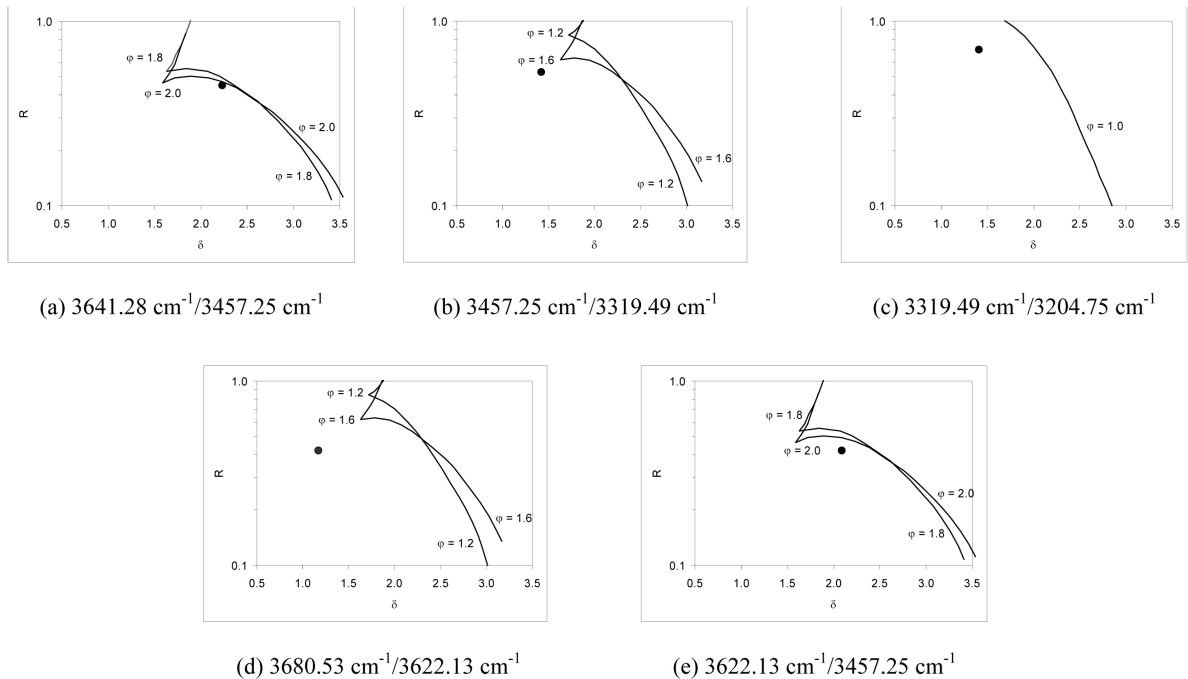
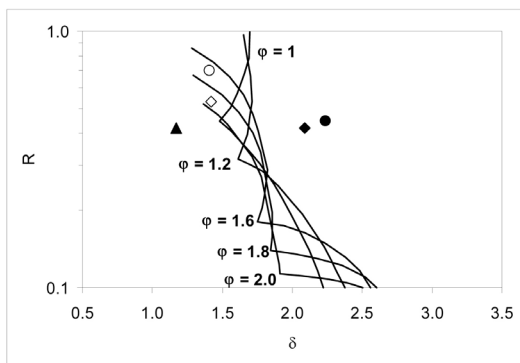


Figure S4. Shoulder limit.

peaks at $3457.25/3319.49\text{ cm}^{-1}$ and $3319.49/3204.75\text{ cm}^{-1}$ are also under the detection limit (Figure S5). As seen in Figure 7 of the paper, the peak at 3319.49 cm^{-1} is barely



- ▲ $3680.53\text{ cm}^{-1}/3622.13\text{ cm}^{-1}$ ◆ $3622.13\text{ cm}^{-1}/3457.25\text{ cm}^{-1}$
 ◇ $3457.25\text{ cm}^{-1}/3319.49\text{ cm}^{-1}$ ○ $3319.49\text{ cm}^{-1}/3204.75\text{ cm}^{-1}$
 ● $3641.28\text{ cm}^{-1}/3457.25\text{ cm}^{-1}$

Figure S5. Detection limit.

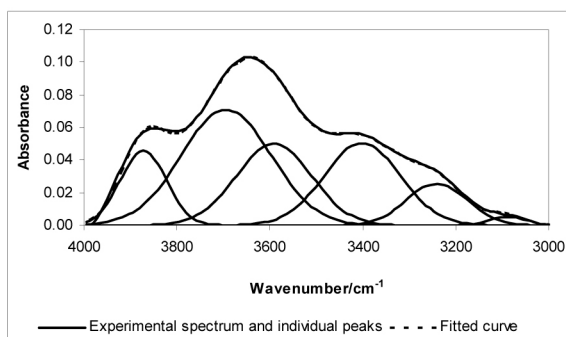
visible in the second derivative and its existence is only confirmed by the fourth derivative.

Using the modified Model I, the peak at 3641.28 cm^{-1} is substituted by two peaks at $3680.53/3622.13\text{ cm}^{-1}$ which are not visually resolved (Figure S4 (d) and (e)). It is interesting to note that the $3622.13/3457.25\text{ cm}^{-1}$ overlapping peaks are beyond the detection limit but do not show up in the second derivative. The reason is that the 3622.13 cm^{-1} peak cannot be detected separately from the 3680.53 cm^{-1} peak, as shown in Figure S5.

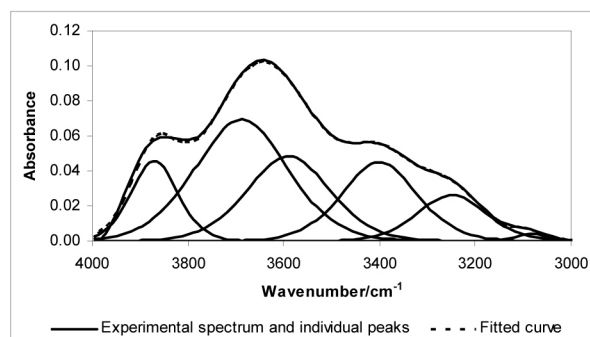
Supplement III: Analysis of Spectrum 3 (14 days ageing at room temperature and under compressive stress of 0.5 GPa)

Curve fitting according to Model I to IV

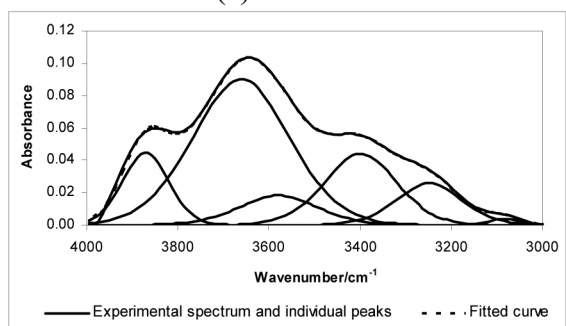
Figure S6 shows the experimental spectrum, together with the separated peaks and the fitted curve, for all curve fitting models. The numerical results are given in Table S4.



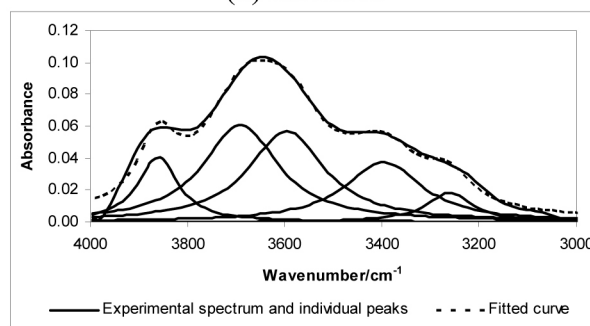
(a) Model I



(b) Model II



(c) Model III



(d) Model IV

Figure S6. Curve fitting results.

Table S4. Numerical results of curve fitting

Initial guess for peak maximum	Parameter	Model I	Model II	Model III	Model IV
3900 cm^{-1}	ν_0 (cm^{-1})	3872.51	3869.89	3870.35	3859.98
	A	0.0456	0.0457	0.0448	0.0409
	s (cm^{-1})	70.24	95.25	90.00	49.60
	s' (cm^{-1})	-	-	109.29	-
3700 cm^{-1}	ν_0 (cm^{-1})	3694.04	3688.00	3660.73	3690.22
	A	0.0710	0.0695	0.0901	0.0612
	s (cm^{-1})	136.61	184.45	181.66	92.45
	s' (cm^{-1})	-	-	250.51	-
3600 cm^{-1}	ν_0 (cm^{-1})	3591.25	3590.32	3579.78	3595.42
	A	0.0500	0.0485	0.0183	0.0572
	s (cm^{-1})	114.34	165.22	164.32	93.59
	s' (cm^{-1})	-	-	168.69	-
3400 cm^{-1}	ν_0 (cm^{-1})	3400.91	3400.17	3398.63	3396.76
	A	0.0505	0.0449	0.0443	0.0377
	s (cm^{-1})	115.74	151.10	148.32	95.94
	s' (cm^{-1})	-	-	151.98	-
3250 cm^{-1}	ν_0 (cm^{-1})	3241.20	3248.77	3248.35	3260.80
	A	0.0257	0.0262	0.0263	0.0184
	s (cm^{-1})	91.96	138.13	137.84	56.73
	s' (cm^{-1})	-	-	135.25	-
3080 cm^{-1}	ν_0 (cm^{-1})	3087.60	3080.93	3081.64	-
	A	0.0053	0.0041	0.0041	-
	s (cm^{-1})	55.67	64.89	64.81	-
	s' (cm^{-1})	-	-	70.28	-

^aUnit (cm^{-1}), ν_0 - peak maximum, s - peak width and s' - the bandwidth term of the Lorentzian part, except A. A - peak height.